JOURNAL OF THEORETICAL
AND APPLIED MECHANICS
https://doi.org/10.15632/jtam-pl/200939
ONLINE FIRST

DAMAGE MECHANISM AND AMPLIFICATION EFFECT OF COMPRESSION FAILURE IN SOFT ROCK WITH INITIAL CRACKS

Senyuan WEN[1], Chaoyi LIAO[2], Shitao YAN[3], Ning LIANG[4*], Tao JIN[4]

[1] *Guangxi Road And Bridge Engineering Group Co., Ltd, Nanning, China*
[2] *Transportation Comprehensive Administrative Law Enforcement Bureau of Guangxi Zhuang Autonomous Region, Nanning, China*
[3] *College of Road and Bridge Engineering, Guangxi Transport Vocational and Technical College, Nanning, China*
[4] *College of Civil and Architectural Engineering, Guangxi University of Science and Technology, Liuzhou, China*

*corresponding author, *liangn5@126.com*

This study presents an approach for characterizing the path of strength failure in pre-cracked soft rocks using the Weibull distribution. Based on the energy obtained from experiments, the damage propagation mechanism and energy dissipation mode of soft rocks were studied. The results indicate that the damage of soft rock forms a diffusion path starting from the two ends of the prefabricated crack, following a characterization model of the Weibull distribution. The dissipation and mutation of energy are the key factors related to the overall instability of the soft rock, and a damage amplification effect area of the soft rock is formed around the prefabricated cracks.

Keywords: soft rock; prefabricated crack; damage; energy characteristics; amplification effect.

1. Introduction

The distribution of soft rocks is extremely extensive worldwide, making these areas important locations for human activities and ecological preservation. In major engineering projects such as excavation in soft rock tunnels, the protection of soft rock slopes, and the reinforcement of foundations, an accurate analysis of the deformation and failure mechanism of soft rocks can provide important guidance for construction methods. The composition and arrangement of soft rock minerals, the initial damage degree, the compressive strength of the rock mass, and the crack pattern collectively determine the overall stability of soft rocks.

Based on the scientific and practical engineering problems aforementioned, many researchers have conducted studies on the failure mechanism of the soft rocks. The difference between the internal friction angle of the soft rock and the cohesive force of particles determines its own elastic modulus and mechanical properties, ultimately leading to different characteristics during its failure (Majedi *et al.*, 2021; Zhang *et al.*, 2022b). Researchers have investigated the correlation between the internal structure and mechanical properties of the soft rock based on the content and particle characteristics of its different components. With the continuous exacerbation of damage, the cracks in soft rocks generate and expand, ultimately leading to a decrease in mechanical performance (Liu *et al.*, 2023; Efimov, 2018). Significant research achievements have been made in relation to the uniaxial compression failure of soft rocks, providing a theoretical basis and experimental methods for the study of damage paths in soft rocks.

The existence of prefabricated cracks usually affects the degradation path and degree of soft rock, and newly generated microcracks mainly occur at both ends of prefabricated cracks (Yuan *et al.*, 2022; Li *et al.*, 2023). Meanwhile, comparing prefabricated cracks at different angles, it was found that the larger the inclination angle, the greater the elastic energy storage of the rock sample. The overall failure mode of rock samples also varies with the angle of

prefabricated cracks (Pan *et al.*, 2023; Zhou *et al.*, 2024). Through numerical experiments, the dynamic process of crack propagation and changes in stress intensity factors can be fully analyzed. The friction coefficient and bonding mode between particles are important physical quantities for the mesoscopic parameters of the soft rock, playing a major role in their mechanical properties (Riazi *et al.*, 2023; Wang *et al.*, 2021; Alenizi *et al.*, 2024). These research findings highlight the impact of pre-cracked soft rocks on the failure process, indicating that initial damage is a disadvantageous factor for soft rock disasters. However, most of the existing research results have focused on the qualitative and variation patterns of prefabricated cracks.

Researchers have also attempted to analyze the evolution of soft rock damage by using quantitative characterization methods. For example, a characterization model of the damage path of the soft rock can be achieved based on the number of sound emissions, energy density, and CT scans. The damage mechanism of soft rock was inferred based on the three-dimensional reconstruction image (Faisal *et al.*, 2017; Gautam *et al.*, 2021; Al-Marzougi, 2018). By utilizing ultrasonic and digital image correlation technologies, the internal pore distribution and stress-strain behavior on the outer surface of soft rocks can be effectively reflected. Ultimately, this enables a quantitative characterization of the three-dimensional space of soft rocks (Abbas *et al.*, 2022; Zhang *et al.*, 2022a; Tian *et al.*, 2024). Therefore, combining qualitative analysis with quantitative characterization is one of the more advantageous methods for studying the failure of soft rocks.

In conclusion, in relation to the existing research results, most studies focus on the analysis of soft rock failure characteristics and physical damage quantities. A series of complex changes triggered by soft rock damage still require further exploration of the related key issues. For example, establishing damage characterization models for soft rocks with different prefabricated crack angles can better predict the failure patterns of rock masses. Therefore, this article focuses on the above issues and presents numerical simulation experiments investigating the compression failure of soft rocks containing prefabricated cracks. The changes in the mechanical and physical parameters of soft rock failure are analyzed based on the experimental results. Based on the internal particle contact and arrangement patterns during the failure process of soft rocks, the study aims to investigate its damage amplification effect.

2. Materials and methods

2.1. Selection of numerical modes

In order to ensure the authenticity of numerical simulations, some parameters can be obtained through indoor experiments. This study focuses on the mudstone sandstone, conducting uniaxial compression failure tests by preparing rock samples with different prefabricated cracks. The experiment adopts a displacement-controlled loading method with a loading speed of 0.03 mm/min. As shown in Fig. 1, the minerals of this type of rock are mainly quartz, feldspar, and mud calcium cement, with a natural density of 2.23 g/cm^3 and an elastic modulus of 4.274 GPa. The rock sample is a standard cylinder with a bottom diameter of 50 mm and a height of 100 mm. The prefabricated crack is semi-transparent; its length, width, and depth dimensions are 10 mm, 2 mm, and 25 mm, respectively. The angle between the prefabricated crack and the horizontal direction is 0°, 15°, 30°, 45°, 60°, 75°, and 90°, respectively.

Fig. 1. Soft rock samples.

2.2. Determination of mesoscopic parameters in numerical experiments

PFC6.0 software was used for the simulations. In order to better simulate the real situation of particles inside the soft rock, the particles in this numerical experiment were all bonded in a parallel manner. In the numerical parallel bonding experiment, the parameters of the specimen include its density and elastic modulus. The mesoscopic parameters of particles include particle size ratio n, linear contact modulus E_c, parallel bonding modulus $\overline{E}_c$, normal bonding strength σ_c, tangential bonding strength τ_c, friction coefficient μ, and stiffness ratio n_k. The parameters of the sample were obtained in indoor experiments, and the mesoscopic parameters of the particles refer to the method introduced by Xiao *et al.* (2019). In order to ensure that the numerical simulation is similar to the indoor experiments, various mesoscopic parameters are continuously fine-tuned. The final parameters used for numerical experiments are shown in Table 1.

Table 1. Values of mesoscopic parameters in numerical experiments.

n	E_c [Pa]	$\overline{E}_c$ [Pa]	τ_c [Pa]	$\overline{\tau}_c$ [Pa]	μ	n_k	n
1.66	1.025E9	6.952E9	3.529E6	7.261E6	0.563	1.356	1.66

2.3. Particle contact model for numerical experiments

In numerical experiments, the connection properties between particles will affect the final accuracy of the calculation results. The interior of the soft rock can generally be divided into two categories, one of which is minerals without cementation, i.e., skeletal particles. These types of particles are relatively stable and do not have adhesive properties. Skeleton particles are usually rigidly connected, and only normal and tangential forces are transmitted between particles. The other category is minerals with cementation, i.e., clay particles. These types of particles have a relatively large composition inside soft rocks and usually play a cementing role between skeleton particles. When clay particles are connected or are inserted between clay particles and skeleton particles, normal force, tangential force, and torque can be transmitted between particles. In addition, these types of particles can maintain their stable state and prevent sliding and loss between particles.

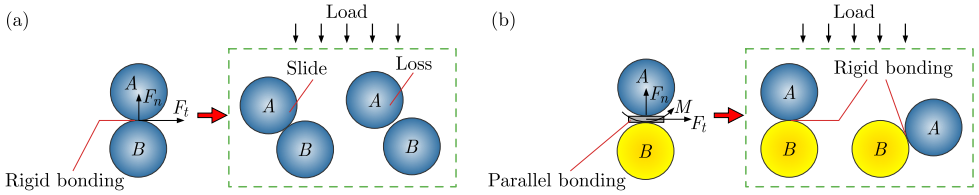

Fig. 2. Particle contact model: (a) rigid connection; (b) parallel bonding.

2.4. Numerical testing methods

This numerical experiment takes the results obtained from indoor experiments as a reference and tries to match them as closely as possible. Based on the mesoscopic parameters obtained above, numerical experiments were modeled and solved using different initial conditions for prefabricated cracks. The experiment is divided into three steps:

– Establishment of the model: the initial physical parameters are defined to form the basic properties of particle flow operations. The number of particles in this experiment is 10000, which meets the numerical test requirements. Based on the contact between particles, as well as between particles and walls, the position of the particles is continuously adjusted until the entire model finally reaches a stable state. For uniaxial compression, after the model is built, the wall on the outer surface of the specimen can be removed to ensure that the confining pressure during the numerical test is kept at zero. After particle generation, prefabricated cracks can form inside the particles. The models of the sample are shown in Fig. 3.

– The bonding properties of particles: particle mesoscopic parameters are set and the parallel bonding properties between particles are repeatedly adjusted. Due to the need to track the cracking between particles in numerical experiments, a measurement circle was added to this experiment, which was used to monitor the deformation and failure displacement of rock samples, and can also track the generation and propagation of cracks. Finally, the fish scripting language was used to set the particle bonding attributes.
– Apply loads and export results: according to the established axial wall model, a displacement-controlled loading method was adopted with a loading speed of 0.03 mm/min. During the loading process, the program recorded the stress and strain data of the specimen in real time, as well as recording the relevant physical quantities of the crack.

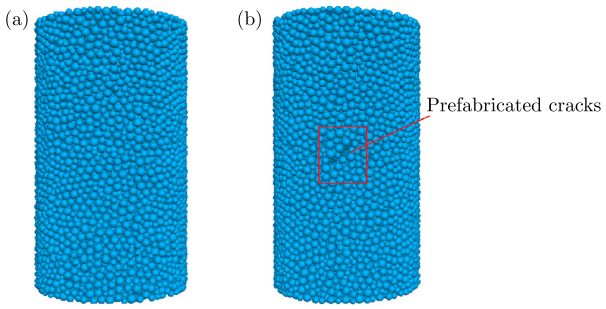

Fig. 3. Sample model for numerical simulation:
(a) no prefabricated crack; (b) including prefabricated crack.

3. Results

3.1. Compressive strength of rock samples with different prefabricated cracks

According to the results of the numerical experiments, the stress-strain curves of different rock samples during the loading process are shown in Fig. 4. In the initial loading stage, as the load increases, the internal particles of the rock sample are continuously compressed. At this point, the rock sample is similar to an isotropic material, and the stress-strain curve exhibits good linear characteristics. When the load reaches the compressive strength of the rock sample, the stress-strain curve loses its original linear variation characteristics and suddenly shows a sharp downward trend. At this point, the rock samples exhibit obvious brittle failure, and their ability to resist external loads becomes weaker. The compressive strength of rock samples with prefabricated cracks is mostly lower than that of rock samples without prefabricated cracks. The larger the angle of the prefabricated crack, the greater the compressive strength of the rock sample. It can be seen that the inclination angle and distribution of the damage location are the key factors affecting the compressive strength of rock samples.

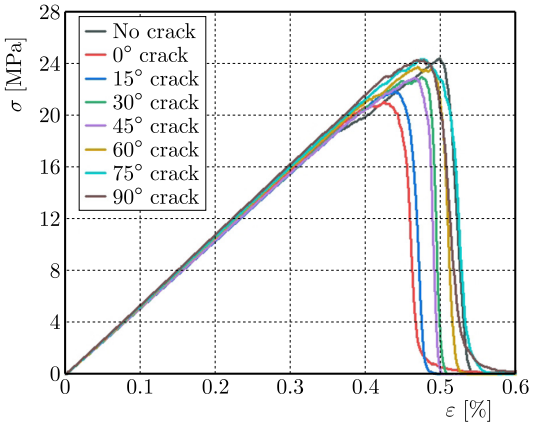

Fig. 4. Stress-strain curves of rock samples with different prefabricated cracks.

3.2. Morphological failure characteristics of rock samples with different prefabricated cracks

Figure 5 shows the final morphology of the rock samples under compression failure. It can be seen that the final failure of the rock sample occurs with the generation of the main crack, and a shear plane is formed along the direction of the main crack. For rock samples containing prefabricated cracks, newly generated cracks start from the two endpoints of the prefabricated cracks and propagate along the direction of the inclination angle. The cracks in rock samples

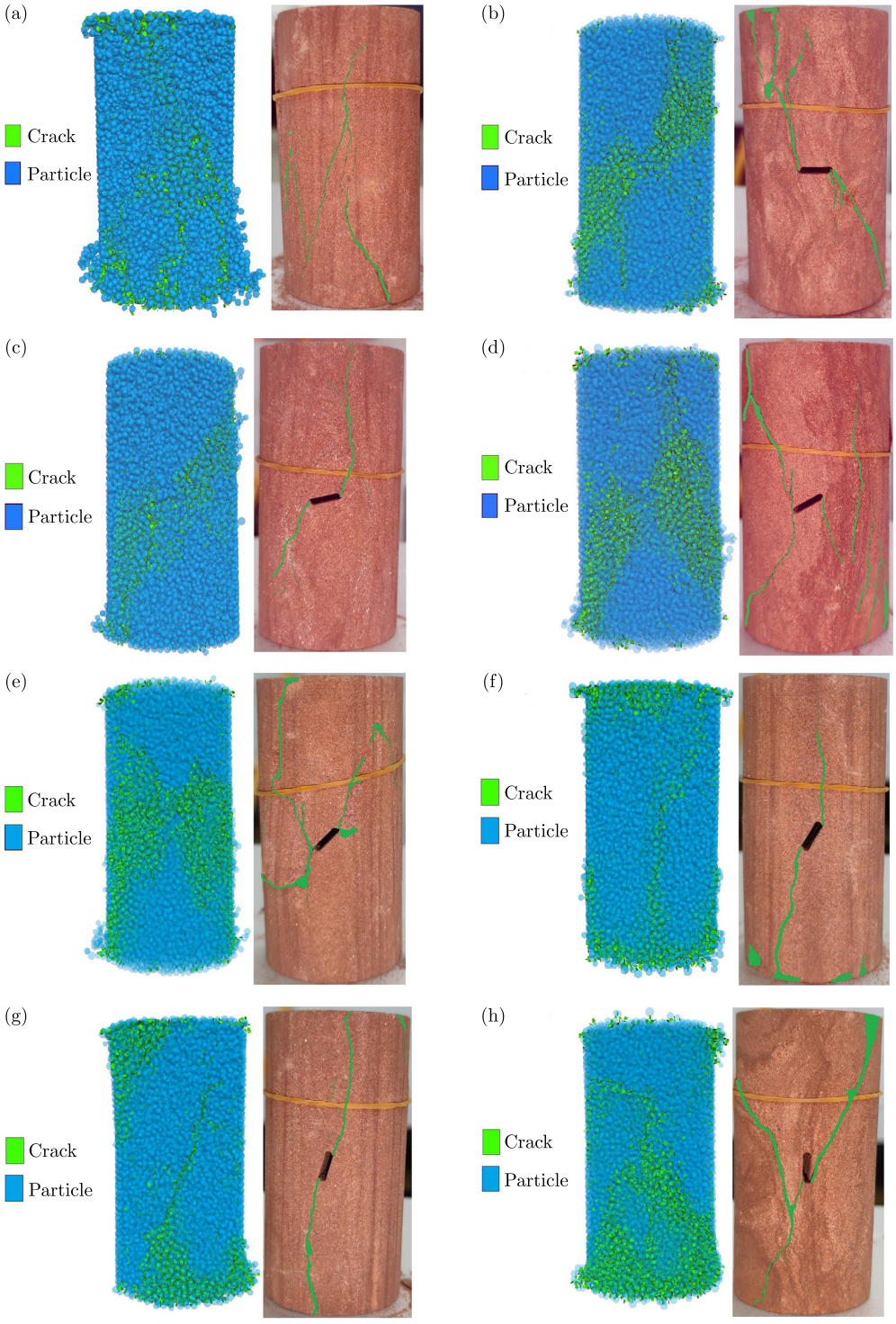

Fig. 5. Final failure mode of rock samples: (a) no crack; (b) 0° crack; (c) 15° crack; (d) 30° crack; (e) 45° crack; (f) 60° crack; (g) 75° crack; (h) 90° crack.

without prefabricated cracks are mainly in the vertical direction. Therefore, the initial damage of the rock sample not only affects the compressive strength of the rock mass, but also guides the failure mode of the rock mass. Meanwhile, for discrete materials such as soft rocks, when the shear plane continues to evolve, the rock mass will exhibit sudden characteristic changes. These sudden changes are the result of the accumulation of internal damage along the main direction in the soft rock.

3.3. Energy characterization of damage process in soft rock with different prefabricated cracks

Assuming that the soft rock and external loading jointly form a complete closed system, it can be considered that the system has no energy exchange with the outside world. From the previous analysis, it can be seen that the soft rock is in the initial stage of particle compaction during loading. For soft rocks, during the compression failure process, there is a continuous exchange of dissipated energy and strain energy. If U represents the total energy input of the loading part to the soft rock, then

$$U = \alpha U_d + \beta U_e, \tag{3.1}$$

where U_d and U_e are the dissipated energy, storage energy, and strain energy of the soft rock, respectively; α and β are the reduction coefficients of energy, which are related to prefabricated cracks and represent different initial damage levels of the soft rock. During uniaxial compression, the rock sample is only subjected to axial stress and the radial stress is 0. Therefore, in the initial stage of loading, there is basically no energy dissipation in the rock sample, and the vast majority is stored as axial strain energy:

$$U = \beta \int_0^{\varepsilon} \sigma \, \mathrm{d}\varepsilon_e, \tag{3.2}$$

where σ is the stress, ε is the total strain, and ε_e is the unit strain. According to the experimental results, it can be seen that when the external load does not reach the compressive strength of the rock sample, the stress-strain curve exhibits obvious linear characteristics. At this point, the rock sample can be approximated as an isotropic material and satisfies Hooke's law. Therefore, the strain energy stored in rock samples can be expressed as follows:

$$U_e = \beta \cdot \frac{1}{2}\sigma \, \mathrm{d}\varepsilon_e = \beta \cdot \frac{1}{2}\sigma\varepsilon = \beta \cdot \frac{E}{2} \cdot \varepsilon^2, \tag{3.3}$$

where E is the elastic modulus of the soft rock. According to Eq. (3.3), the accumulation of energy in rock samples comes from the application of loads. At this point, the rock sample converts external loads into strain energy and continuously completes the storage. When the load reaches the compressive strength of the rock sample, the stored strain energy of the rock sample reaches its maximum value, which is inevitably accompanied by the release of energy. Therefore, after the peak strength, the rock sample releases strain energy in the form of dissipated energy.

The total energy curves of different pre-cracked rock samples during the loading process are shown in Fig. 6. In the initial stage of loading, as the load continues to increase, the strain of the rock sample also increases. The strain and strain energy stored in rock samples follow a quadratic exponential distribution. When the load exceeds the compressive strength of the rock sample, the total energy of the rock sample reaches a stable state, and the rock sample exhibits a sudden failure characteristic. This is due to the strain energy being converted into dissipated energy in a short period of time. The release of dissipated energy in rock samples leads to rapid brittle failure.

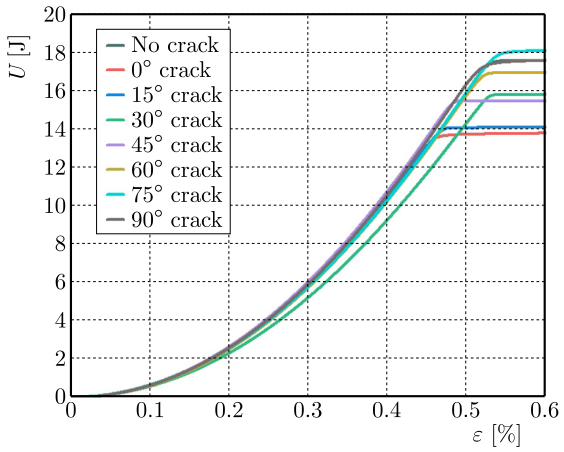

Fig. 6. Total energy curves of different pre-cracked rock samples during loading.

4. Discussion

4.1. Distribution characterization model of soft rock damage caused by different prefabricated cracks

For soft rock, its internal structure is complex and uneven. The Weibull distribution can effectively describe this random strength characteristic, and the parameters in its probability density function can reflect the physical and mechanical properties of the soft rock, such as material uniformity, defect distribution, etc. By assuming that the strength of the soft rock follows the Weibull distribution, it can better capture the laws of strength changes in the soft rock under different prefabricated crack conditions, and more accurately predict the failure mode and mechanical behavior of the soft rock.

As a discrete medium, the soft rock is initially distributed with pores and fractures of varying sizes. Therefore, the rock sample exhibits varying degrees of initial damage, and the presence of prefabricated cracks determines the different states of initial damage. Assuming that the strength of the soft rock follows the Weibull distribution, the relevant probability density function $P(\varepsilon)$ is as follows:

$$P(\varepsilon) = \frac{m}{F}\left(\frac{\varepsilon}{F}\right)^{m-1} \exp\left[-\left(\frac{\varepsilon}{F}\right)^{m}\right], \tag{4.1}$$

where ε represents the strain of the soft rock, while m and F represent the Weibull distribution parameters – these represent the physical and mechanical properties of the soft rock. The ratio of the number of microelements N_e that cause failure in the soft rock to the total number of microelements N in the soft rock is defined as the damage variable, which can be expressed as follows:

$$D = \frac{N_e}{N} = \frac{\int\limits_0^{\varepsilon} NP(x)\,\mathrm{d}x}{N} = \frac{N\left\{1-\exp\left[-\left(\frac{\varepsilon}{F}\right)^{m}\right]\right\}}{N} = 1-\exp\left[-\left(\frac{\varepsilon}{F}\right)^{m}\right]. \tag{4.2}$$

According to the acoustic emission results obtained from numerical experiments, it can be seen that the amount of ringing is mostly concentrated near the peak stress, and the amount of ringing in other processes is very small. The entire acoustic emission curve shows a clear peak and a sharp decline on both sides. This distribution feature is very similar to the damage variable characterization equation aforementioned. If the damage distribution of the acoustic emission curve is similar to that of a rock sample, the characterization equation of the fitted acoustic emission ringing number N is as follows:

$$N = D_0 + a \cdot \exp\left[\frac{(\varepsilon_c-\varepsilon)^2}{2b^2}\right], \tag{4.3}$$

where D_0 is the initial damage value, ε_c is the peak strain, ε is the strain, and a and b are the distribution parameters, respectively. Therefore, the related parameters of different pre-cracked soft rock damage fitted by the above equation are shown in Table 2.

Table 2. Values of mesoscopic parameters in numerical experiments.

Parameter	No crack	0°	15°	30°	45°	60°	75°	90°
D_0	0.052	0.046	0.047	0.050	0.047	0.045	0.069	0.043
ε_c	0.517	0.453	0.461	0.488	0.482	0.499	0.517	0.501
a	19.954	21.174	22.542	19.032	24.137	19.953	18.874	12.957
b	0.005	0.005	0.004	0.004	0.004	0.006	0.005	0.005

According to the data in Table 2, it can be seen that different prefabricated cracks have varying degrees of influence on the initial damage, peak strain, and distribution parameters of the soft rock. In addition, the peak strain without prefabricated cracks is larger than that with prefabricated cracks. This indicates that soft rocks with a smaller amount of initial damage have a stronger strain capacity and a greater compressive performance. The peak strain of the soft rock with 0° prefabricated cracks is the smallest. This result has also been validated in numerical simulation and indoor experiments.

4.2. Amplification criteria of soft rock damage caused by different prefabricated cracks

According to the experimental results and the comprehensive analysis above, the application of load causes the soft rock to absorb a large amount of energy and store it inside the rock mass. This causes the continuous adjustment of the internal structure of the soft rock. A nonlinear dynamic mechanism is formed between the soft rock and the external loads. The fluctuation and mutation of energy ultimately cause an amplification effect of soft rock damage, leading to the overall failure of the soft rock. At this point, the soft rock exhibits a strong damage amplification effect, and its internal particles continuously recombine. The damage and failure process of rock samples without prefabricated cracks and with 45° prefabricated cracks is illustrated in Figs. 7 and 8.

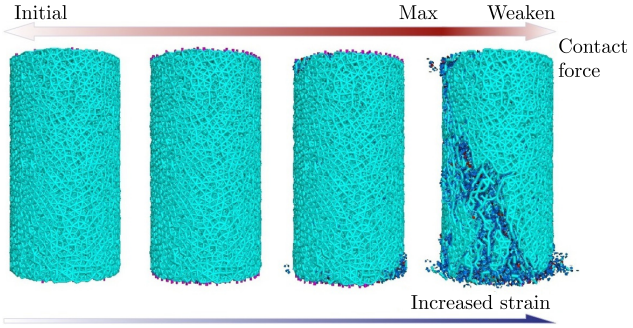

Fig. 7. Particle contact force during damage process of rock samples without prefabricated cracks.

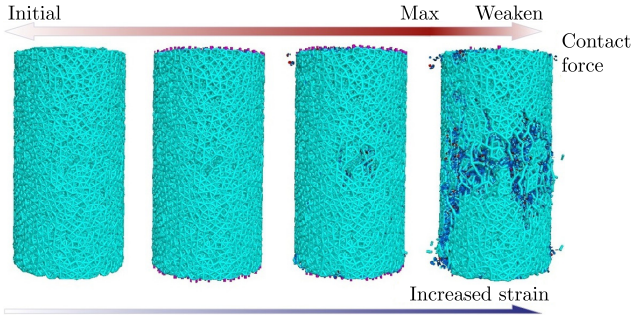

Fig. 8. Particle contact force during damage process of 45° pre-cracked rock samples.

When the load continues to increase, the contact force between particles reaches the limit state, and the bearing capacity of particles cannot resist more loads. Figure 9 shows the damage amplification effect model of the internal structure of soft rocks. At this point, the particles inside the rock sample mainly reflect two possible adjustment forms. One form transfers the load to nearby particles, whereby the connections between nearby particles become tighter. Another form involves the connection performance between particles being disrupted, resulting in the release of load and the formation of local damage. When the vast majority of particles inside the rock sample reach the limit state of bearing capacity, these tightly connected particles instantaneously fail, releasing the load they bear. At this point, it is the concentrated manifestation of the amplification effect of rock damage, which is the key node for the overall failure of the soft rock.

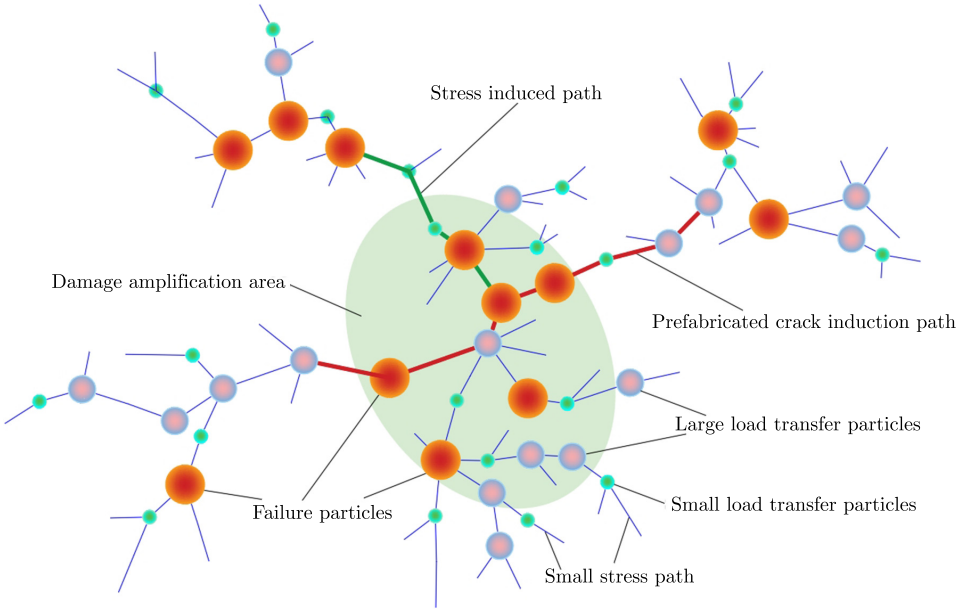

Fig. 9. Damage amplification effect model for the internal structure of soft rocks.

4.3. Exploration of numerical simulation on soft rock damage path and amplification effect

Numerical simulation can deeply explore the mechanical behavior and damage evolution process of the soft rock under different prefabricated crack conditions. Więckowski (2004) introduced the application of the material point method in large strain industrial and geomechanical problems. Similar to the research content of this article, both emphasize the relationship between the microstructure and the macroscopic mechanical response of materials. Sokołowski and Kamiński (2018) used the stochastic finite element method (SFEM) to study the mechanical properties of composite materials with defects. This is consistent with the method used in this article to consider the influence of prefabricated cracks on the mechanical properties of soft rocks, which focuses on the impact of internal defects or damage on the overall performance of the material. In addition, some researchers (Riazi *et al.*, 2023; Sun *et al.*, 2023; Wu *et al.*, 2023) found, through particle flow software or XFEM methods, that the pre-splitting angle of rocks has a significant impact on the mechanical properties and crack propagation of the model. This complements the research presented in this article, emphasizing the advantages of numerical simulation in revealing the internal mechanical mechanisms of rocks.

5. Conclusions

This article proposes a method that uses the Weibull distribution to characterize the strength failure path of pre-fractured soft rock, and studies the damage propagation mechanism and en-

ergy dissipation mode of the soft rock based on numerical and indoor experiments. The dissipation and mutation of energy have been identified as key factors in the overall instability of the soft rock, and it has been found that there is a damage amplification effect zone around prefabricated cracks. The research conclusions are as follows:

- At the initial stage of loading, the stress-strain curves of different pre-fractured soft rocks exhibit good linear characteristics. After the peak stress, the curve becomes dispersed. The compressive strength of soft rock decreases with the decrease in the precast crack angle. The damage of the soft rock propagates along the direction of prefabricated cracks.
- Soft rocks exhibit evolution laws of energy absorption, dissipation, and abrupt changes during compression. The damage changes in the soft rock follow the Weibull distribution, exhibiting obvious nonlinear and non-equilibrium phase transition characteristics. The smaller the angle of prefabricated cracks, the lower the peak stress of the soft rock. This indicates a faster failure rate and more pronounced brittle characteristics, revealing the key role of energy dissipation and abrupt changes in overall instability.
- The damage and destruction of soft rocks have a significant amplification effect, which is a concentrated manifestation of their internal particle connections and continuous adjustments. The load is transmitted or released by particles inside the soft rock, ultimately forming a damage amplification effect zone of overall failure. Elucidating the relationship between soft rock damage, internal particle connection adjustment, and load transfer and release provides a new perspective for the stability analysis of soft rock engineering.

Acknowledgments

This research was supported by the Guangxi Science and Technology Program (no. AD23026265, no. AD21220126), the Scientific Research Basic Ability Improvement Project of Young and Middle-aged Teachers in Guangxi Colleges and Universities (no. 2022KY1140).

References

1. Abbas, H.A., Mohamed, Z., & Mohd-Nordin, M.M. (2022). Characterization of the body wave anisotropy of an interbedded sandstone-shale at multi orientations and interlayer ratios. *Geotechnical and Geological Engineering*, *40*(7), 3413–3429. https://doi.org/10.1007/s10706-022-02096-8
2. Alenizi, F.A., Mohammed, A.H., Alizadeh, S.M., Gohari, O.M., & Motahari, M.R. (2024). Appraisal of rock dynamic, physical, and mechanical properties and forecasting shear wave velocity using machine learning and statistical methods. *Journal of Applied Geophysics*, *223*, Article 105216. https://doi.org/10.1016/j.jappgeo.2023.105216
3. Al-Marzouqi, H. (2018). Digital rock physics: Using CT scans to compute rock properties. *IEEE Signal Processing Magazine*, *35*(2), 121–131. https://doi.org/10.1109/MSP.2017.2784459
4. Efimov, V.P. (2018). Features of uniaxial compression failure of brittle rock samples with regard to grain characteristics. *Journal of Mining Science*, *54*(2), 194–201. https://doi.org/10.1134/S1062739118023545
5. Faisal, T.F., Awedalkarim, A., Chevalier, S., Jouini, M.S., & Sassi, M. (2017). Direct scale comparison of numerical linear elastic moduli with acoustic experiments for carbonate rock X-ray CT scanned at multi-resolutions. *Journal of Petroleum Science and Engineering*, *152*, 653–663. https://doi.org/10.1016/j.petrol.2017.01.025
6. Gautam, P.K., Dwivedi, R., Kumar, A., Verma, A.K., Singh, K.H., & Singh, T.N. (2021). Damage characteristics of Jalore granitic rocks after thermal cycling effect for nuclear waste repository. *Rock Mechanics and Rock Engineering*, *54*(1), 235–254. https://doi.org/10.1007/s00603-020-02260-7
7. Li, B., He, Y.Z., Li, L., Zhang, J.X., Shi, Z., & Zhang, Y.P. (2023). Damage evolution of rock containing prefabricated cracks based on infrared radiation and energy dissipation. *Theoretical and Applied Fracture Mechanics*, *125*, Article 103853. https://doi.org/10.1016/j.tafmec.2023.103853

8. Liu, J., Wang, B., Wang, Y.S., Shi, L., Xie, X.K., & Lan, J. (2023). Experimental study on a granular material-filled lining in a high ground-stress soft-rock tunnel. *Applied Sciences*, *13*(24), Article 13326. https://doi.org/10.3390/app132413326

9. Majedi, M.R., Afrazi, M., & Fakhimi, A. (2021). A micromechanical model for simulation of rock failure under high strain rate loading. *International Journal of Civil Engineering*, *19*(5), 501–515. https://doi.org/10.1007/s40999-020-00551-2

10. Pan, X.W., Wan, L., Jiang, T., Jia, Y.C., & Zhang, S. (2023). Experimental study on strength and failure characteristics of mortar specimens with prefabricated cracks under uniaxial and triaxial stress. *Frontiers in Materials*, *10*, Article 1287623. https://doi.org/10.3389/fmats.2023.1287623

11. Riazi, E., Yazdani, M., & Afrazi, M. (2023). Numerical study of slip distribution at pre-existing crack in rock mass using extended finite element method (XFEM). *Iranian Journal of Science and Technology, Transactions of Civil Engineering*, *47*(4), 2349–2363. https://doi.org/10.1007/s40996-023-01051-8

12. Sokołowski, D. & Kamiński, M. (2018). Computational homogenization of carbon/polymer composites with stochastic interface defects. *Composite Structures*, *183*, 434–449. https://doi.org/10.1016/j.compstruct.2017.04.076

13. Sun, X., Li, W., Zhang, C., Zhang, G., & Xia, Z. (2023). Mechanical behaviors and fracture characteristics of sandstone combinations with different pre-crack angles. *KSCE Journal of Civil Engineering*, *27*(12), 5388–5400. https://doi.org/10.1007/s12205-023-1941-8

14. Tian, H., Shu, X., Chen, W., Tan, X., Yang, D., & Tian, Y. (2024). Impact of structural anisotropy on compressive creep behaviors of composite rocks based on digital image correlation technology. *Bulletin of Engineering Geology and the Environment*, *83*(8), Article 299. https://doi.org/10.1007/s10064-024-03792-w

15. Wang, H., Wang, Y.Y., Yu, Z.Q., & Li, J.G. (2021). Experimental study on the effects of stress-induced damage on the microstructure and mechanical properties of soft rock. *Advances in Civil Engineering*, *2021*(1), Article 6696614. https://doi.org/10.1155/2021/6696614

16. Więckowski, Z. (2004). The material point method in large strain engineering problems. *Computer Methods in Applied Mechanics and Engineering*, *193*(39–41), 4417–4438. https://doi.org/10.1016/j.cma.2004.01.035

17. Wu, Y., Ma, D.D., Hu, X.J., Hao, Y., Liu, C.H., & Zhou, H.Y. (2023). Numerical simulation on the mechanical and fracture behavior of bedding argillaceous sandstone containing two pre-existing flaws. *Theoretical and Applied Fracture Mechanics*, *127*, Article 104047. https://doi.org/10.1016/j.tafmec.2023.104047

18. Xiao, Z.Q., Wang, X., Tang, D.S., Dong, Q.Y., Jiang, Y.N., Yang, K., Cao, T.T., & Deng, Z. (2019). Microscopic fabric characteristics of typical red soft rock in Badong Formation under uniaxial compression test (in Chinese). *Coal Geology & Exploration*, *47*(6), 103–114.

19. Yuan S.X., Jiang, T., Lei, J.H., & Cui, C.H. (2022). Experimental study on fracture characteristics of rock-like material with prefabricated cracks under compression shear. *Scientific Reports*, *12*(1), Article 2809. https://doi.org/10.1038/s41598-022-06712-8

20. Zhang, K., Jiang, Z., Liu, X.H., Zhang, K., & Zhu, H. (2022a). Quantitative characterization of the fracture behavior of sandstone with inclusions: Experimental and numerical investigation. *Theoretical and Applied Fracture Mechanics*, *121*, Article 103429. https://doi.org/10.1016/j.tafmec.2022.103429

21. Zhang, W., Zhao, T., & Yin, Y. (2022b). Prefabricated fractured rock under stepwise loading and unloading. *Journal of Theoretical and Applied Mechanics*, *60*(1), 167–179. https://doi.org/10.15632/jtam-pl/145582

22. Zhou, J., Wang, K.Z., Zhou, W.D., Yao, Y.L., & Xie, T. (2024). Uniaxial compressive damage characteristics of rock-like materials with prefabricated conjugate cracks. *Applied Sciences*, *14*(2), Article 20823. https://doi.org/10.3390/app14020823

Manuscript received November 4, 2024; accepted for publication February 6, 2025; published online April 10, 2025.